

G. GUMIENNY*[‡], T. GIĘTKA**

CONTINUOUS COOLING TRANSFORMATION (CCT) DIAGRAMS OF CARBIDIC NODULAR CAST IRON

WYKRESY CTP_c ŻELIWA SFEROIDALNEGO Z WĘGLIKAMI

This work presents continuous cooling transformation diagrams for different kinds of carbidic nodular cast iron. We investigated the cast iron, chemical composition of which in nodular cast iron allows the obtainment of a metal matrix which consists of: pearlite, upper bainite and its mixture with lower bainite, ausferrite and martensite when the casts were cooled in the mold. The influence of the rate of cooling on the obtained microstructure and hardness of the casts was shown. The work describes the influence of the alloy additives on the curves of austenite decomposition in the carbidic nodular cast iron. Diagrams were plotted which enable an understanding of the kinetics of the transformations of austenite in carbidic nodular cast iron. The diagrams also indicate the possibility of obtaining pearlite, bainite, martensite and ausferrite with the established chemical composition and the wall thickness of the cast.

Keywords: carbidic nodular cast iron, bainite, ausferrite, continuous cooling transformation diagrams

W pracy przedstawiono wykresy CTP_c różnych rodzajów żeliwa sferoidalnego z węglkami. Zbadano żeliwo o składzie chemicznym zapewniającym uzyskanie w żeliwie sferoidalnym osnowy metalowej złożonej z: perlitu, bainitu górnego oraz jego mieszaniny z dolnym, ausferytu i martenzytu przy studzeniu odlewów w formie. Pokazano wpływ szybkości studzenia na uzyskiwaną mikrostrukturę i twardość odlewów. Opisano wpływ dodatków stopowych na krzywe rozpadu austenitu w żeliwie sferoidalnym z węglkami. Opracowane wykresy umożliwią poznanie kinetyki przemian austenitu w żeliwie sferoidalnym z węglkami oraz ocenę możliwości uzyskania perlitu, bainitu, martenzytu i ausferytu przy zadanym składzie chemicznym oraz grubości ścianki odlewu.

1. Introduction

Previous research on the subject indicates that in nodular non-alloy cast iron the bainitic or ausferritic microstructure can be obtained by hardening through isothermal holding in the range of austenite → bainite transformation [1, 2]. The end of isothermal holding before the beginning of carbide precipitation from carbon supersaturated austenite and ferrite produces the ausferritic microstructure. Subsequently, austempered ductile iron (ADI) is obtained, which is known in different types [3]. It is used for machine units and devices used in the conditions of wear and adhesive wear. It is possible to obtain ausferrite in non-alloy cast iron only for the casts whose wall thickness is less than 8 mm [4]. In the case of casts with thicker walls, elements which increase the hardenability of the cast iron should be added. Elements such as Mo, Cr, Cu, Ni cause displacement of the curve of the beginning of austenite decomposition in the direction of the longer periods of time and that nickel has the most intensive influence. The influence of copper on austenite stability is less intensive. In order to obtain the pearlitic metal matrix, Cu and Ni are added to cast iron. For this reason the concentration of Mn is increased by a

maximum of 0.8%. Chromium and molybdenum are carbide forming elements, but to some extent they dissolve in austenite, influencing its stability. The influence of molybdenum is also typical, in that it increases the stability of austenite in the range of its transformation to pearlite. However, it does not have an important influence on its stability in the bainitic range. The schematic influence of Mo on austenite stability in cast iron is presented in Figure 1 [5].

It follows from this that for the rate of cooling of the cast v , in cast iron without a Mo additive, the austenite is subjected to transformation into a mixture of ferrite and pearlite. However, in cast iron with a Mo additive, the transformation is one into bainite or ausferrite. Obtaining the bainitic or ausferritic microstructure is conditioned by the content of Mo and other alloy additives, e.g. Cu and Ni, the correct concentration of which enables the obtention of the above mentioned microstructure without ferrite or pearlite inclusion [5÷9]. In order to obtain the martensitic microstructure it is necessary to add elements which increase the hardness in such a quantity that when cooling the cast in the mold, it would be possible to obtain the rate of cooling equal to, or larger than, the critical one, both in the range of austenite transformation into pearlite and into bainite.

* DEPARTMENT OF MATERIALS ENGINEERING AND PRODUCTION SYSTEMS, LODZ UNIVERSITY OF TECHNOLOGY, 1/15 STEFANOWSKIEGO STR., 90-924 ŁÓDŹ, POLAND

** MATERIAL ENGINEERING UNIT, MECHANICAL ENGINEERING DEPARTMENT, UNIVERSITY OF TECHNOLOGY AND LIFE SCIENCE IN BYDGOSZCZ, 7 PROF. S. KALISKIEGO STR., 85-796 BYDGOSZCZ, POLAND

[‡] Corresponding author: grzegorz.gumienny@p.lodz.pl

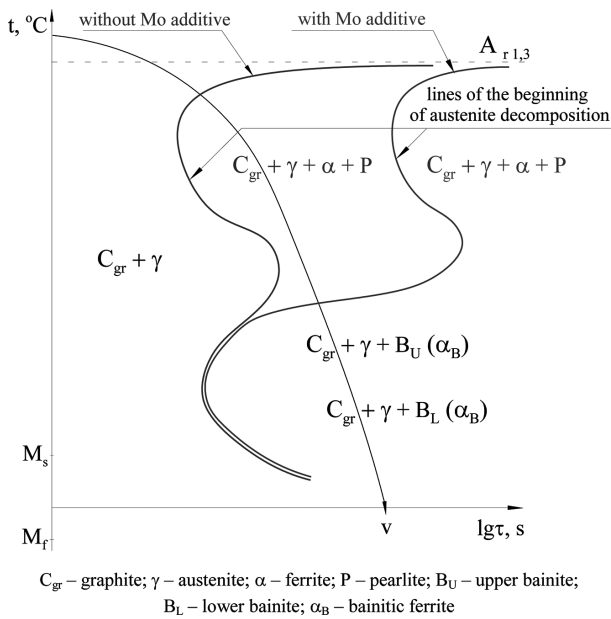


Fig. 1. The scheme of molybdenum influence on the curves of the beginning of austenite decomposition in cast iron [4]

Research detailing time-temperature-transformation diagrams of the nodular cast iron is presented, among others, in work [10]. On the basis of TTT diagrams systems that support the production of ductile iron or other alloys are created [11]. The continuous cooling transformation diagrams for carbidic nodular cast iron have not been drawn so far. It is for this reason the aim of this research was to devise continuous cooling transformation diagrams of carbidic nodular cast iron and to present the influence of molybdenum, chromium, nickel and copper on the curves of decomposition of austenite in the tested cast iron. The continuous cooling transformation diagrams in this paper should be helpful when selecting the chemical composition of nodular cast iron for obtaining the unwrought (without thermal treatment) different microstructure of the metal matrix.

2. Methodology of the research

The cast iron used in the research was melted in an induction furnace with the capacity of 30 kg. The nodularising was carried out using the Inmold method which is based on the use of master alloy in the gate assembly of the mold.

The chemical composition of certain types of cast iron was tested on an emissive spectrometer with spark excitation SPECTROMAXx by SPECTRO Analytical Instruments GmbH (see Table 1).

The maximum concentration of P and S was 0.04% and 0.01% respectively.

The microstructure of cast iron was tested on the polished sections etched by nital under $\times 1000$ magnification using an Eclipse MA200 metallographic microscope by Nikon.

The surface percentage was investigated using the NIS Elements BR software designed to analyze the image.

The chemical composition of the carbidic nodular cast iron was selected in order to guarantee the obtainment of the metal matrix consisting of: pearlite, upper bainite, mixture of upper and lower bainite, ausferrite and martensite after cooling the cast in the sand mold (without thermal treatment). With regards to the high "vulnerability" of the cast iron on the rate of cooling, the sample cast was made in the shape of

a step with a wall thickness of 3, 6, 12 and 25 mm in order to estimate the microstructure of the initial cast iron. To carry out the dilatometric tests, casts in the form of a roll with the diameter of 18 mm were made, and the specimens of $\varphi 3$ mm and length 10 mm were scattered. The microstructure of the cast iron in the cast in the shape of a roll was similar to that obtained in the sample cast with the wall thickness of 12 mm.

TABLE 1
Chemical composition of the tested kinds of carbidic nodular cast iron

No	Chemical composition, %						
	C	Si	Mn	Cr	Mo	Ni	Cu
	3.78	2.26	0.24	0.89	0.03	0.78	1.50
	3.29	2.35	0.07	0.03	1.90	0.94	0.02
	3.83	2.36	0.06	0.03	2.00	1.62	0.02
	3.75	2.40	0.33	0.51	1.41	0.03	1.03
	3.72	2.32	0.31	0.50	0.02	3.85	1.03

A high speed quenching dilatometer RITA L78 by LINSEIS was used to make the continuous cooling transformation diagrams. This is presented in Figure 2 (a, b).

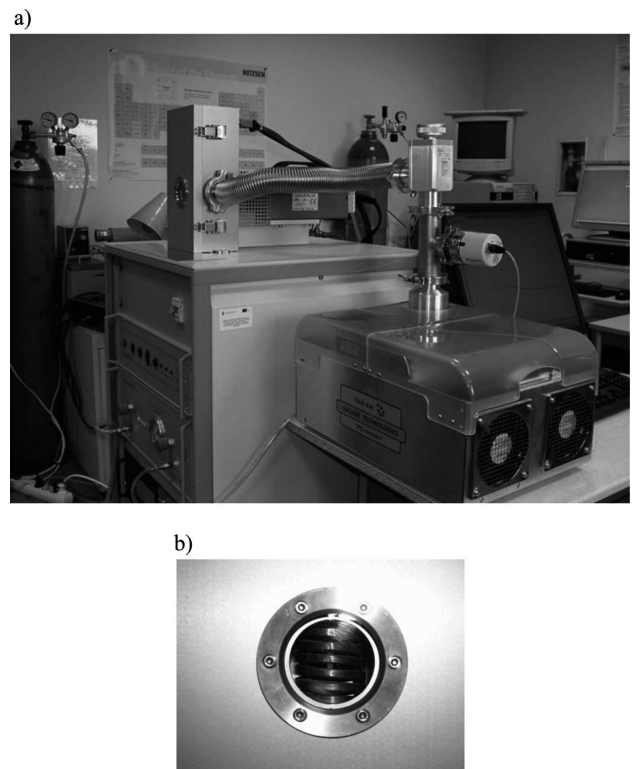


Fig. 2. Dilatometer Linseis Rita L78 (a), the specimen heated inductively (b)

The continuous cooling transformation diagrams were made on the basis of the analysis of the dilatometric curves obtained for different constant cooling rates of the specimens from the temperature of austenitizing to the ambient temperature. The analysis was based on determining the temperature points of the beginning and the end of the phase transition of the austenite. The rates of cooling fell into a wide range from dozens $^{\circ}\text{C/s}$ to some $^{\circ}\text{C/min}$. In terms of the graphitization of

the cast iron during the heating and the annealing (austenitizing), each specimen for the dilatometric tests was used only once.

Before the tests, dilatometric measures were carried out for each type of specimen (heating with the rate $q = 5^\circ\text{C}/\text{min}$) in order to select the austenitizing parameters ($920^\circ\text{C}/30\text{ min}$).

When the specimens had been measured, two further measures of hardness HV30 were carried out, their average is presented in the continuous cooling transformation diagrams.

3. The results of the research

Figure 2 (a, b) shows the microstructure of the initial cast iron for the dilatometric tests which contains about 0.9% Cr; 0.8% Ni and 1.5% Cu (Tab. 1, No 1) in the cast with extreme wall thickness, i.e. 3 and 25 mm. The conducted experiments showed that the microstructure of the cast with the wall thickness of 6 and 12 mm was similar to the microstructure of the cast with the wall thickness of 3 and 25 mm respectively.

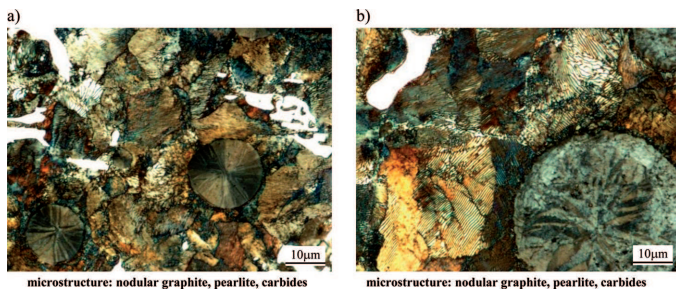


Fig. 3. Microstructure of initial carbidic nodular cast iron containing about: 1.0% Cr; 0.8% Ni; 1.5% Cu in the cast with wall thickness of 3 mm (a) and 25 mm (b)

It follows from this that the microstructure of the cast iron after cooling in the mold is pearlitic, with carbides in the tested range of the chemical composition and the wall thickness of the casts. More refinement of the microstructure components of the cast iron can be seen in Fig. 2a, which is caused by a higher rate of cooling of the cast with the wall thickness of 3 mm in comparison to the cast with thicker walls.

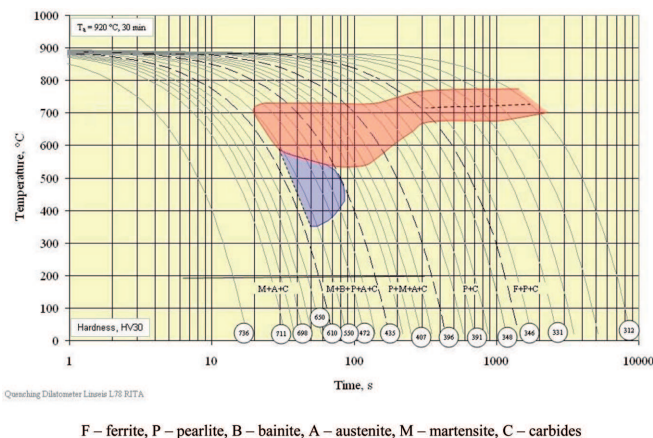


Fig. 4. CCT diagram of carbidic nodular cast iron with the chemical composition: 3.78% C; 2.26% Si; 0.24% Mn; 0.89% Cr; 0.78% Ni; 1.50% Cu

Figure 3 presents the continuous cooling transformation diagram for the cast iron containing about 0.9% Cr, 0.8% Ni and 1.5% Cu (Tab. 1, No 1). The specimens cooled with the

rate of cooling: 6, 10, 15, 20, 30, 45, 60, 75, 90, 120, 150, 180, 210, 240, 300, 375, 450, 600, 750, 900, 1050, 1200, 1380, 1620, 3000 and $6000^\circ\text{C}/\text{min}$ were used to draw it.

As indicated in the diagram presented in Fig. 3, the cast iron with the chemical composition given above the martensitic matrix was obtained at cooling rate of more than $900^\circ\text{C}/\text{min}$. For the rate of cooling in the range of $450\div 750^\circ\text{C}/\text{min}$ the microstructure of the metal matrix of the examined nodular cast iron consists of a mixture of pearlite, bainite and martensite. The precipitations of martensite in the pearlitic matrix were also seen in the specimens which were cooled at the cooling rate of $120\div 375^\circ\text{C}/\text{min}$. The cast iron which was cooled in the range of $60\div 90^\circ\text{C}/\text{min}$ had a metal matrix consisting of pearlite and carbides. At a smaller rate of cooling, sheathings of ferrite are formed around the precipitations of the nodular graphite. The surface percentage of the ferrite increased, together with the decrease in the rate of cooling.

Fig. 4 (a, b) shows the microstructure of the initial cast iron containing about 1.9% Mo and 0.9% Ni (Tab. 1, No 2), obtained after the cooling in the mold.

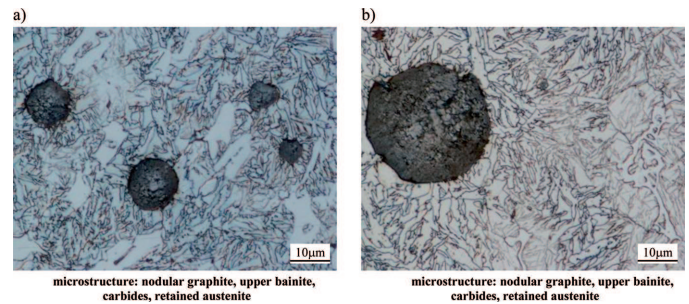


Fig. 5. Microstructure of initial carbidic nodular cast iron containing about 2.0% Mo and 1.0% Ni in the casts with the wall thickness of 3 mm (a) and 25 mm (b)

For the casts with the given chemical composition and the tested wall thickness, the upper bainite and the carbides in the metal matrix are obtained unwrought. This is caused by the common impact of Mo and Ni on the stability of the austenite. The surface percentage of the carbides was from 8 to 4% in the cast with the wall thickness 3 and 25 mm respectively.

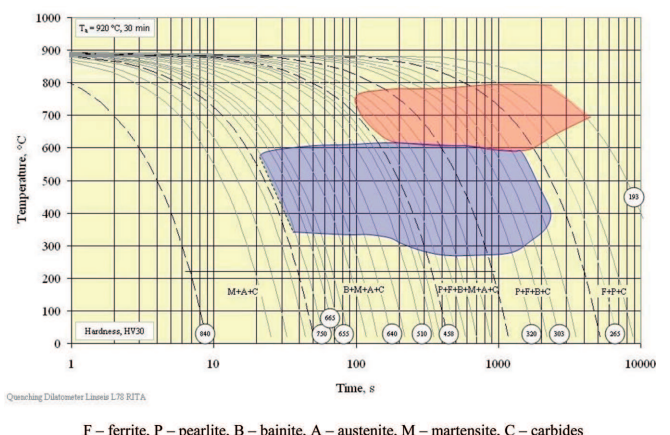


Fig. 6. CCT diagram of carbidic nodular cast iron with the chemical composition: 3.29% C; 2.35% Si; 0.07% Mn; 1.90% Mo; 0.94% Ni

Figure 5 presents a continuous cooling transformation diagram for the nodular cast iron containing about: 1.9% Mo and 0.9% Ni (Tab. 1, No 2). The specimens which were cooled

with the rate of cooling: 3, 6, 8, 10, 15, 20, 24, 30, 45, 60, 75, 90, 105, 120, 135, 150, 180, 240, 300, 375, 450, 600, 675, 750, 900, 1050, 1200, 1620, 2100 and 6000°C/min were used to draw it.

From this diagram, it is clear that the molybdenum and nickel, with concentrations of about 1.9% and 0.9% respectively, caused the movement of the pearlitic transformation zone in the direction of longer periods of time in comparison to the cast iron without Mo. The austenite stability in the bainitic range is similar to that in the cast iron without the Mo additive. This indicates that molybdenum increases the austenite stability essentially in the range of its transformation into pearlite. However, it does not have much influence on its stability in the bainitic transformation. At the same time, this element caused the expansion of the bainitic transformation range in the direction of longer times (lower rates of cooling). The temperature at the beginning of the martensitic transformation is higher in comparison to the previously described kind of cast iron. It is caused by the lack of copper and a low concentration of manganese. The presence of the above mentioned elements causes a decrease in the temperature M_s . The presence of about 1.9% Mo did not have any influence on the decrease in temperature of the beginning of the martensitic transformation because the majority of its atoms form part of the carbides. It is for this reason that its concentration in the austenite is low [12].

The bainitic microstructure without the precipitations of ferrite and pearlite was obtained in the cast iron being cooled at the rate of 105÷900°C/min. Apart from the bainite the metal matrix contained the carbides and the martensite whose surface percentage decreased when the rate of cooling also decreased. At smaller rates of cooling, ferrite and pearlite appeared in the cast iron matrix. Martensite precipitations were observed for the specimens cooled at a rate no lower than 30°C/min. At the rate of cooling in the range of 10÷24°C/min the microstructure of the metal matrix consisted of a mixture of the ferrite, pearlite and bainite. At lower rates of cooling, the ferrite and pearlite was observed in the tested nodular cast iron.

Figure 6 (a, b) presents the microstructure of the initial carbidic nodular cast iron containing about 2.0% Mo and 1.6% Ni.

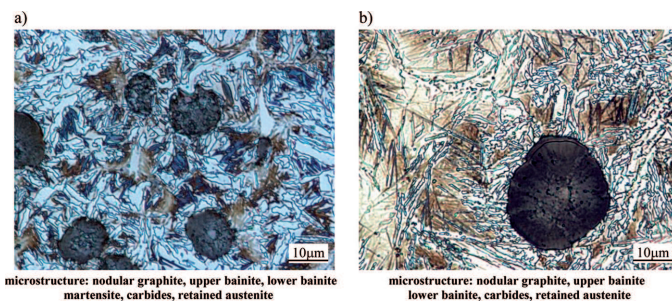


Fig. 7. Microstructure of initial carbidic nodular cast iron containing about 2.0% Mo and 1.6% Ni in the casts with wall thickness of 3 mm (a) and 25 mm (b)

The increase in the nickel content with a similar content of molybdenum caused the presence of upper and lower bainite and the carbides in the metal matrix of the initial cast iron used for the dilatometric tests. In the casts with a wall thickness of 3 mm in the metal matrix, a small quantity of martensite additionally appeared. This is caused by a higher rate of cooling in comparison to the cast with a wall thickness of 25 mm. The research showed that in order to eliminate the

martensite in the thin-wall casts, it is necessary to decrease the content of nickel to about 1.3%. The surface percentage of the carbides was similar to the cast iron containing 1.9% Mo and 0.9% Ni.

Figure 7 presents the continuous cooling transformation diagram of the cast iron containing about 2.0% Mo and 1.6% Ni (Tab. 1, No 3). The following rates of cooling were applied: 6, 7, 8, 10, 12, 15, 20, 24, 30, 36, 45, 60, 75, 90, 105, 120, 150, 180, 240, 300, 360, 396, 450, 510, 600, 750, 900 and 1620°C/min.

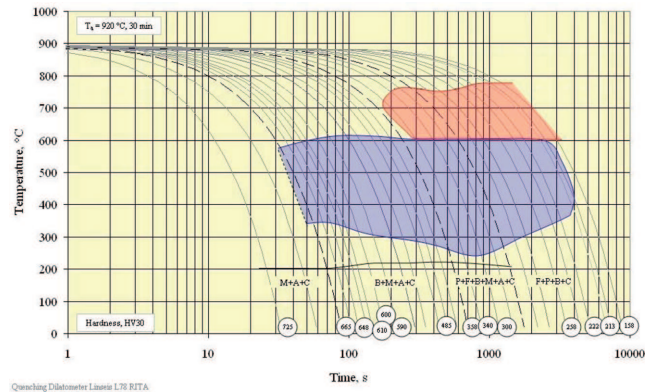


Fig. 8. CCT diagram of carbidic nodular cast iron with the chemical composition: 3.83% C; 2.36% Si; 0.06% Mn; 2.00% Mo; 1.62% Ni

From CCT diagram presented in Figure 7 it is clear that the increase of the nickel content in 0.7% at a similar molybdenum content caused the increase in the austenite stability in the range of transformation in pearlite and bainite. The decrease of the temperature of the $\gamma \rightleftharpoons \alpha$ transformation was caused by the pearlitogenic activity of the nickel. With regard for the movement of the curve of the beginning of the austenite decomposition in the bainitic zone to the direction of longer periods of time, the cast iron is characterized by increased quenching. The temperature of the end of the $\gamma \rightarrow$ bainite transformation is lower in comparison to the cast iron containing about 0.9% Ni. The bainitic-martensitic microstructure in the cast iron in question was obtained by a rate of cooling in the range of 90÷750°C/min.

The increase in the content of nickel also caused a decrease in temperature M_s , and thus, a decrease in the hardness of the tested cast iron as a result of increased levels of retained austenite.

The microstructure of the initial cast iron for the dilatometric tests, containing approximately 1.4% Mo; 0.5% Cr and 1.0% Cu, is presented in Figure 8 (a, b).

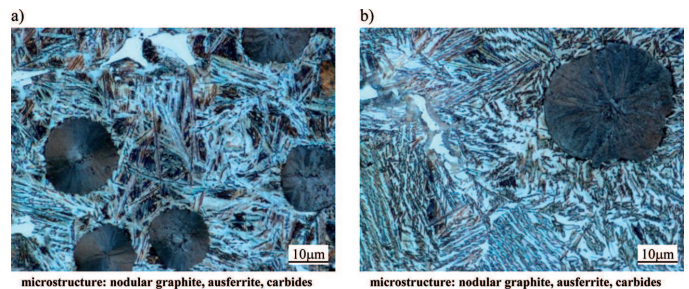
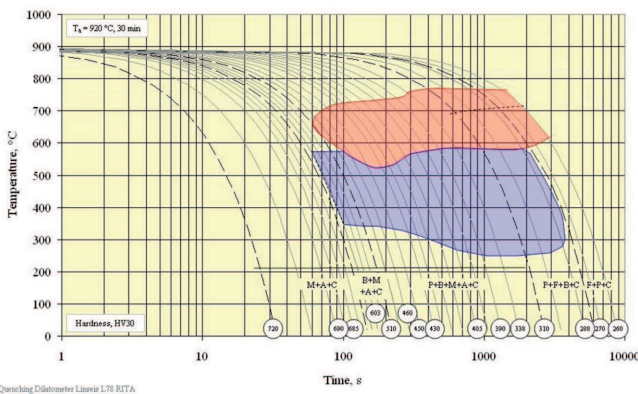


Fig. 9. Microstructure of initial carbidic nodular cast iron containing about: 1.5% Mo; 1.0% Cu and 0.5% Cr in the casts with the wall thickness of 3 mm (a) and 25 mm (b)

From these results, it can be deduced that the ausferritic microstructure in the carbidic nodular cast iron can be obtained by the given combination of Mo, Cu and Cr in the casts with the wall thickness of 3÷25 mm cooled in the mold. The surface percentage of the carbides was 5% and 3% in the cast with the wall thickness of 3 and 25 mm respectively.

Figure 9 presents the continuous cooling transformation diagram for the cast iron, the chemical composition of which allows the obtention of ausferrite without any thermal treatment (Tab. 1, No 4). The following rates of cooling were used to plot the presented CCT diagram: 6, 8, 10, 15, 20, 30, 40, 50, 60, 75, 90, 105, 120, 150, 180, 210, 240, 270, 300, 330, 360, 402, 450, 510, 600, 900 and 1620°C/min.



F – ferrite, P – pearlite, B – bainite, A – austenite, M – martensite, C – carbides

Fig. 10. CCT diagram of carbidic nodular cast iron with the chemical composition: 3.75% C; 2.40% Si; 0.33% Mn; 0.51% Cr; 1.41% Mo; 1.03% Cu

From these results, it follows that the zone of the pearlitic transformation is moved into the direction of the shorter time periods in comparison to the types of cast irons previously described. It is caused by a decreased concentration of molybdenum and the Cu additive which increase the austenite stability in the range of the pearlitic transformation to a lower degree than nickel. The copper influence on the beginning of the austenite decomposition in the range of the bainitic transformation is more intense than that of nickel. In the cast iron previously discussed, the martensitic microstructure was obtained by a rate of cooling in the range of 360÷1620°C/min. The pearlite precipitations occurred in the metal matrix of the cast iron which was cooled with a rate equal to 210°C/min or less. The sheathings of ferrite around the nodular graphite appeared in the cast iron which was cooled with a range equal to or less than 20°C/min.

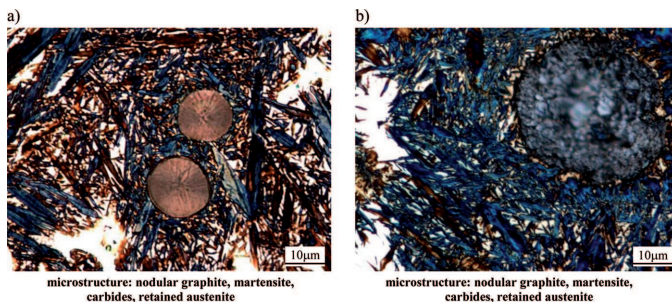
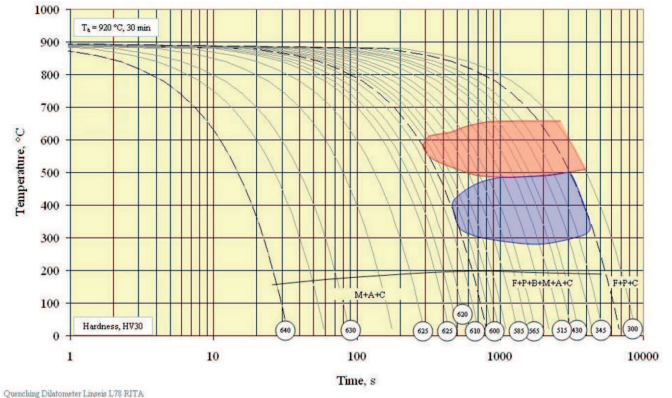


Fig. 11. Microstructure of initial carbidic nodular cast iron containing about 3.8 Ni; 1.05 Cu and 0.5% Cr in the casts with the wall thickness of 3 mm (a) and 25 mm (b)

Figure 10 (a, b) presents the microstructure of the initial cast iron for the dilatometric tests containing approximately 0.5% Cr; 3.8% Ni and 1.0% Cu (Tab. 1, No 5).

From test, it was possible to observe that in the metal matrix of cast iron, apart from the carbides, there is exclusively martensite and retained austenite. The surface percentage of the carbides was 5% and 3% in the cast with the wall thickness of 3 and 25 mm respectively. The continuous cooling transformation diagram for this type of cast iron are presented in Figure 11. The following rates of cooling of the specimens were used: 6, 8, 10, 12, 15, 17, 20, 24, 30, 34, 40, 48, 54, 60, 66, 75, 90, 105, 120, 180, 300, 600, 900 and 1620°C/min.



F – ferrite, P – pearlite, B – bainite, A – austenite, M – martensite, C – carbides

Fig. 12. CCT diagram of carbidic nodular cast iron with the composition: 3.72% C; 2.32% Si; 0.31% Mn; 0.50% Cr; 3.85% Ni; 1.03% Cu

What is visible here is that the common additives Ni, Cu and Cr caused a significant increase in the austenite stability both in the pearlitic and the bainitic zones. The martensitic microstructure with the retained austenite, without the precipitation of other phases, was obtained in the carbidic nodular cast iron, discussed above, at a rate of cooling in the range of 66÷1620°C/min. For the rate in the range of 10÷60°C/min, ferrite, pearlite and bainite appeared too in the metal matrix. High concentrations of nickel and the copper additive caused a decrease in the temperature of the austenite-ferrite transformation in comparison to the previously described types of cast iron.

4. Conclusions

The research carried out for this paper allowed the plotting of continuous cooling transformation diagrams of carbidic nodular cast iron. Obtainment of the above mentioned microstructure was possible due to the use of the right composition of chromium, molybdenum, copper and nickel. The typical influence of Mo on austenite decomposition curves was confirmed. This influence consists in intensive increases of its stability in the pearlitic transformation and a much less pronounced one in the bainitic transformation. The diagrams give a better understanding of the kinetics of the austenite decomposition in carbidic nodular cast iron. It can find its use in the selection of the chemical composition of nodular cast iron in order to obtain the pearlitic, bainitic, martensitic or ausferritic microstructure at established rates of cooling (cast wall thickness).

REFERENCES

- [1] E. Guzik, The Processes of Cast Iron Refining, Archives of Foundry Engineering, 2001, Monography No 1M [in Polish].
- [2] E. Guzik, W. Kapturkiewicz, J. Lelito, Principles of Obtaining of the Ausferritic Cast Iron. International Science Conference, on the topic of ADI – foundry offer for the designers and casts users. Krakow, 23-24.IX.2000, p. I/11 [in Polish].
- [3] E. Guzik, Ausferritic Cast Iron and Its Kinds, Productive Systems Optimization Tendencies in Foundries, Team work under the editorship of Stanisław Pietrowski, Katowice – Gliwice 2010, pp. 105-110 [in Polish].
- [4] S. Pietrowski, Nodular Cast Iron with the Structure of Bainitic Ferrite with Austenite or Bainitic, Material Science Archives **4**, 18, 253-273 (1997) [in Polish].
- [5] G. Gumienny, Bainitic Nodular Cast Iron with Carbides Obtaining with Use of Inmold Method, Archives of Foundry Engineering **9**, 3, 243-248 (2009).
- [6] G. Gumienny, Bainitic-martensitic Nodular Cast Iron with Carbides, Archives of Foundry Engineering **10**, 2, 63-68 (2010).
- [7] S. Pietrowski, G. Gumienny, Crystallization of Nodular Cast Iron with Carbides, Archives of Foundry Engineering **8**, 4, 236-240 (2008).
- [8] S. Pietrowski, G. Gumienny, Carbides in Nodular Cast Iron with Cr and Mo, Archives of Foundry Engineering **7**, 3, 223 (2007).
- [9] M. Ferry, W. Xu, Microstructural and Crystallographic Features of Ausferrite in As-cast Gray Iron, Materials Characterization **53**, 43-49 (2004).
- [10] I. Olejarczyk-Woźnińska, A. Adrian, H. Adrian, B. Mrzygłód, Parametric Representation of TTT Diagrams of ADI Cast Iron, Archives of Metallurgy and Materials **57**, 2, 613-617 (2012).
- [11] Z. Górny, S. Kluska-Nawarecka, D. Wilk-Kołodziejczyk, Heuristic Models of the Toughening Process to improve the Properties of Non-Ferrous Metal Alloys. Archives of Metallurgy and Materials **58**, 3, 849-852 (2013) DOI: 10.2478/amm-2013-0085.
- [12] S. Pietrowski, G. Gumienny, Microsegregation in Nodular Cast Iron with Carbides, Archives of Foundry Engineering **12**, 4, 127-134 (2012).